Strain induced coexistence of monoclinic and charge ordered phases in $La_{1-x}Ca_xMnO_3$

P. R. Sagdeo, Shahid Anwar, and N. P. Lalla
UGC-DAE Consortium for Scientific Research, University Campus, Khandwa Road, Indore 452017, India
(Received 28 September 2006; published 29 December 2006)

Coexistence of charge-ordered (CO) and monoclinic (M) phases has been investigated in $La_{1-x}Ca_xMnO_3$ ($x=0.6$, 0.67, and 0.7). For this purpose, pellets and their corresponding powdered samples have been studied employing low-temperature powder x-ray diffraction down to 87 K and transmission electron microscopy down to 109 K. Diffraction studies have revealed that the coexistence of M and CO phases occurs only in pellet samples and not in the powdered versions of the same samples. The powders, which have exactly the same composition as their corresponding pellets, show only CO phases. The observed coexistence of M and CO phases in pellets is not due to compositional inhomogeneity within the grain but due to the presence of intrinsic strain in the pellets that is being imposed by the grain boundary network on the grains of the *Pnma* phase. The occurrence of monoclinic phase has been attributed to the possible softening of C_{44} elastic modulus of the pseudocubic phase.

DOI: 10.1103/PhysRevB.74.214118 PACS number(s): 61.10.Nz, 75.47.Lx, 68.37.Lp, 61.50.Ks

I. INTRODUCTION

The perovskite manganites $A_{1-x}B_xMnO_3$ (A=rare earths and B=alkaline earths) exhibit interconnected magnetic, electronic, and structural phase transitions that do show coexistence of competing phases of nano- to micro-meter length scales[1–3] in polycrystalline and single-crystal samples.[4–9] Recently coexistence of charge-ordered and monoclinic phases[7,8] has also been reported in bulk lanthanum calcium manganese oxide (LCMO). The issue of phase coexistence is important in order to understand the physics of colossal magnetoresistive (CMR) materials.[10] The origin of nanometer- and micrometer-scale phase coexistence has been attributed to various reasons such as chemical disorder (charge inhomogeneity) of substituents at A and B sites, the random field, and to the localized and broad electronic wave functions (L-B model).[10–15] On the other hand, theory incorporating primarily the structural aspects such as elastic energy landscapes (strain fields), predict[16] both nanometer- and micrometer-sized coexisting phases. An important point to note is that most of the micron-sized phase coexistence has been found in samples prepared out of bulk samples such as ceramics or single crystals.[6,7] In bulk samples, strain fields are expected to be spontaneously present as a result of their processing. It is quite likely that the observed[7,8] coexistence of M and CO phases might be due to the presence of strain in the sample.[16,17] But to date there is no direct experimental investigation reporting the correlation between the long-range strain in the bulk manganites and the occurrence of phase coexistence. Such studies are important from the structural phase characterization point of view. Most of the basic physical property studies are done on polycrystalline pellets, but results are very frequently interpreted based on the structural phase characterizations done on powders. Further, looking into the theoretical expectations,[16,17] the structural phase transformation and hence the electrical and magnetic behavior may have an appreciable difference in pellet and powdered versions of the manganites.

II. EXPERIMENTAL DETAILS

Keeping the above in view, we have carried out comparative structural studies on a series of overdoped (more than half doped) $La_{1-x}Ca_xMnO_3$ ($x=0.6$, 0.67, and 0.7) manganites taken in the form of hard sintered pellets (15 mm $\phi \times 3$ mm, pelletized at 50–200 kilo N/cm^2) and its corresponding powders. These were prepared through the solid-state reaction route. In this composition range, coexistence of M and CO phases has already been reported.[7] The powders were made by gentle grinding of a part of the same pellets for 2–3 min in an agate mortar and pestle. Structural studies were done using low-temperature x-ray diffraction (XRD) and transmission electron microscopy (TEM) down to 87 K and 109 K, respectively. Details of the sample preparation method used in the present studies are given in Ref. 18. Thin samples for TEM observations were prepared following the standard technique using ion milling. Details of TEM sample preparation together with other bulk characterizations can be found in Ref. 19.

III. EXPERIMENTAL RESULTS

A. X-ray diffraction results

Figures 1(a) and 1(b) show selected peaks of room-temperature XRD of (a) pellets and (b) the corresponding powders of the LCMO samples studied in the present investigation. The presence of broad peaks appearing as shoulders on the lower angle sides of the (202)/(040) peaks of the *Pnma* phase can be clearly seen in the XRD profiles of the pellet samples. Such shoulders were also present around other major peaks of the *Pnma* phase, such as (240), (242), and (161). Surprisingly, the signature of these shoulders was completely absent from the XRD profiles of corresponding powdered samples, see Fig. 1(b). Figures 2(a) and 2(b) show the same XRD peaks of (a) pellets and (b) the powders as in Fig. 1 but collected at 87 K. It can be clearly noticed that the shoulderlike peaks, as indicated by arrows in the XRD profiles corresponding to pellets, are now well separated from the peaks corresponding to the *Pnma* phase. The peaks due to *Pnma* phase have split into (602) and (040) for $x=0.67$ and (802) and (040) for $x=0.70$ of the CO phase occurring at low temperatures. In the case of powders, only (602) and

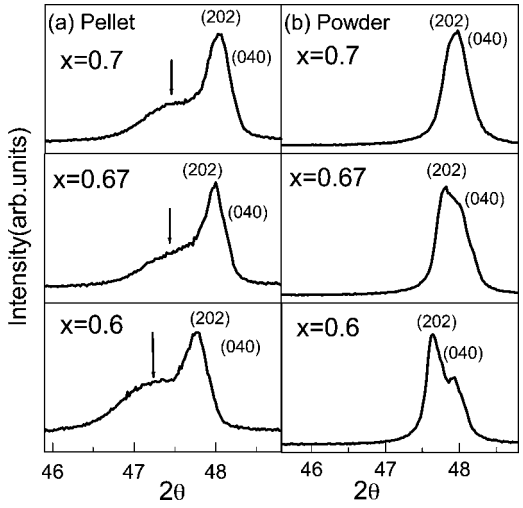

FIG. 1. Room-temperature powder XRD profiles of $La_{1-x}Ca_xMnO_3$ (x=0.6, 0.67, and 0.7) samples in pellet (a) and powder (b) forms. It can be clearly seen that the shoulderlike broad peaks indicated by arrows present in the lower angle side of the XRD profile corresponding to pellets have completely vanished, in contrast to the powdered samples. These broad peaks indicate the presence of strain.

(040) splitting is observed, and no other peaks grow at the position of the broad peak as seen for pellets. Details of the evolution taking place at low temperatures in the XRD profile for x=0.67 and x=0.70 can be seen in Figs. 3(a) and 3(b). A comparison of XRD profiles in Figs. 2(a) and 2(b) shows that intensity ratio of (602) to (040) in pellets is invariably higher than that of the corresponding powders. This feature is rather more vivid for the x=0.7 sample but it is present for all compositions studied in the present investigation. It appears roughly to be proportional to the intensity of the broad peak. This extra intensity at (602) {or (802)} in pellets is basically due to its superposition with the peak being split from the broad peak and approaching from the lower angle side. For identifying the phase giving rise to the broad peak in the XRD pattern, transmission electron microscopic imaging and diffraction was carried out at various temperatures from room temperature down to 109 K. Electron diffraction was carried out in selected area diffraction (SAD) and convergent beam electron diffraction (CBED) modes. This phase is identified[7,8] as a monoclinic (M) phase, with lattice parameters a=5.47±0.05 Å, b=7.62±0.05 Å, c=5.44±0.05 Å, and β=91.8±0.5° at 109 K. Using multiple peak fittings, we could successfully fit these XRD profiles based on the above two phases, see Fig. 4. The splitting of $(\bar{2}02)$ and (040) peaks of M-phase can be clearly seen. As temperature decreases splitting between these two peaks increases and the (040) of the M phase finally coincides with (602) of the CO phase. Thus the M phase coexists with the charge-ordered (CO) phase at low temperatures in bulk sample, see Fig. 5. The peaks due to M phase have been indicated. Superlattice peaks corresponding to charge ordering in samples with x=0.67 and 0.70 are indicated in the insets of Fig. 5.

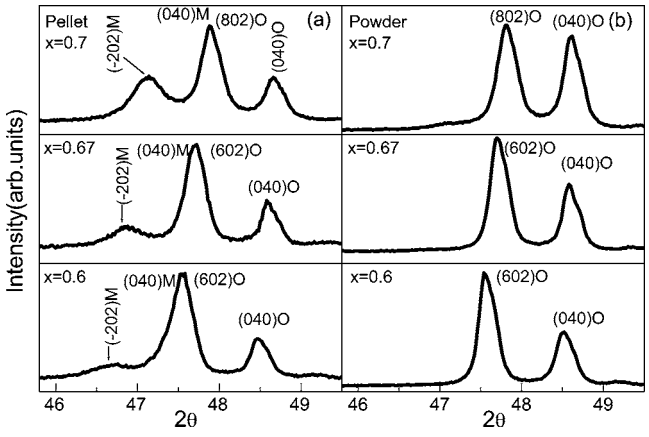

FIG. 2. Low-temperature (87 K) powder XRD profile between 2θ=46°–49° of $La_{1-x}Ca_xMnO_3$ (x=0.6, 0.67, and 0.7) samples in pellet (a) and powder (b) forms. It can be clearly seen that the shoulderlike feature present in the lower angle side of the XRD profile corresponding to pellets is well resolved at 87 K. This peak is mainly due to $(\bar{2}02)$ reflection of the monoclinic phase and thus represents the coexistence of monoclinic (M) and charge-ordered (CO) phases. The complete absence of M phase from the powdered sample signifies the importance of the role of strain in coexistence of M and CO phases.

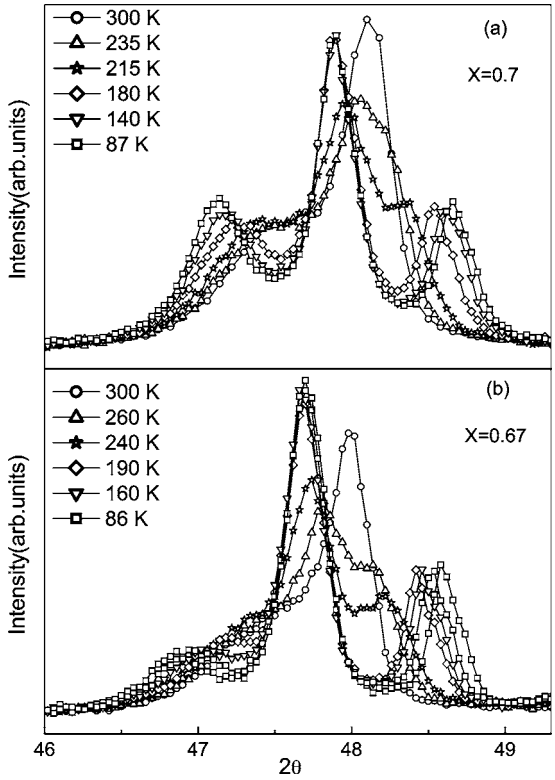

FIG. 3. Temperature evolution of the XRD profile of pellet samples for (a) x=0.7 and (b) x=0.67 from room temperature down to 87 K.

B. Transmission electron microscopy results

Figures 6(a)–6(d) show TEM micrographs taken at 300 K, 240 K, 215 K, and 109 K, respectively, for the x

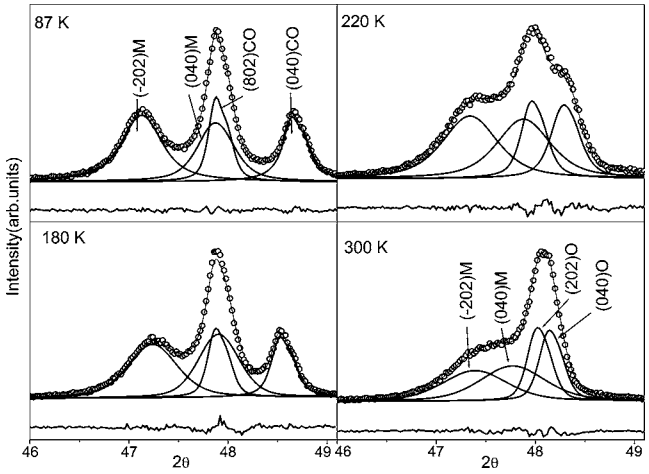

FIG. 4. Multipeak fitting of the XRD profiles of pellet of $x=0.7$ sample at 87 K, 180 K, 220 K, and 300 K. Arrows indicate the indices of peaks due to M and CO phases. It can be noticed that the FWHM of the peaks due to M phase decreases with decreasing temperature and the (040) peak of monoclinic almost merges with the (602) peak of CO phase.

$=0.67$ sample. The presence of a sharp demarcation boundary separating the M and CO phases can be seen in the low-temperature micrographs. This boundary fades with increasing temperature and at about 240 K it almost disappears. The SAD from upper (M phase) region does not show any superlattice spot, but only a deformed (although not very obvious) reciprocal lattice corresponding to the monoclinic phase, see Fig. 6(e). But the lower region does show superlattice spots due to charge ordering, see Fig. 6(f). Figure 6(f) has been taken from a region common to both M and CO phases. The splitting of fundamental reciprocal lattice spots, as indicated by arrows, appears due to the relative shift of the reciprocal lattice spots of the M and CO phases in its a^*-c^* plane. These splittings are visual evidence of the coexistence of M and CO phases, particularly in the present case where the β parameter of the monoclinic phase is close to 90° and hence the obliquity of the monoclinic lattice is visually not very clear in the SAD pattern shown in Fig. 6(e). Figures 7(a) and 7(b) show the CBED patterns taken at 109 K across the sharp demarcation line respectively from the CO and M phases. CBED patterns were used for direct comparison of b parameters of the two phases by measuring diameters of first-order Laue zone (FOLZ) rings. We could very accurately calibrate the camera length for the CBED patterns and obtain the lattice spacing corresponding to (040) plane. The b parameter will be four times the lattice spacing corresponding to its (040) plane, i.e., 7.62 ± 0.05 Å. For calibration, the camera length lattice spacing corresponding to the (040) peak of the CO phase (1.871 Å), as obtained from the XRD data given in Fig. 2(a), was used as an internal standard. This indicates that the (040) peak of the monoclinic phase lies very close to the (602) peak of the CO phase, i.e., the middle peak in the XRD profiles shown in Figs. 2 and 3.

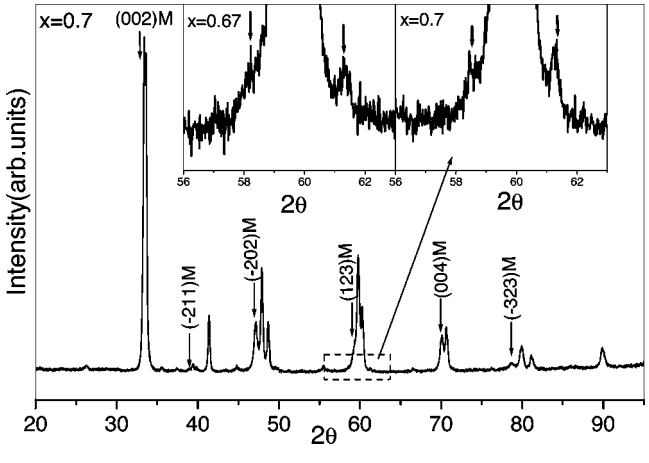

FIG. 5. Full XRD profile of $x=0.7$ sample at 87 K exhibiting the coexistence of monoclinic (M) and charge-ordered (CO) phases. The XRD peaks corresponding to M phase have been indexed and indicated by arrows. The insets show selected superlattice peaks due to charge ordering in $x=0.67$ and 0.70 samples.

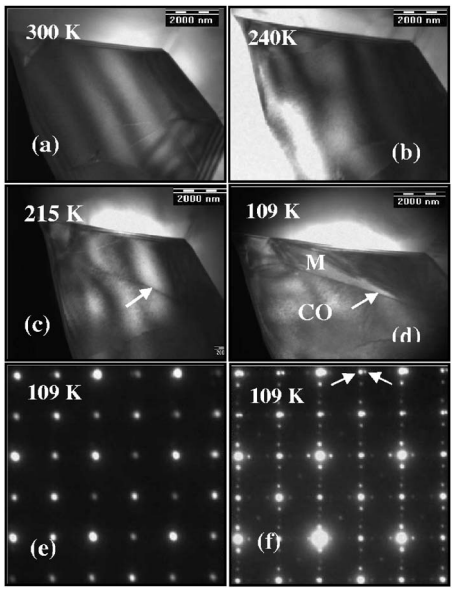

FIG. 6. TEM micrographs of pellet sample for $x=0.67$ at (a) 300 K, (b) 240 K, (c) 215 K, and (d) 109 K. In 109 K micrograph, the coexistence of M and CO phases has been indicated. The SAD pattern corresponding to M phase is shown in (e) and that of from the region common to M and CO phases is shown in (f). The split spots, as indicated by arrows, are due to M and CO phases.

It can be noticed that these coexisting regions of monoclinic and charge-ordered phases are of several microns, much bigger than the expected.[10,13] These regions were examined through energy dispersive x-ray analysis (EDAX) and were found to be of the same chemical composition. The most important and interesting point to note is that the features in 109 K micrograph were found to exactly reproduce during repeated heating-cooling cycles between room temperature and 109 K. This is indicative of the fact that the observed coexistence is biased by a physical parameter other than the sample temperature. If the temperature had been the only parameter, the microstructure should have shown variations after each thermal cycling.

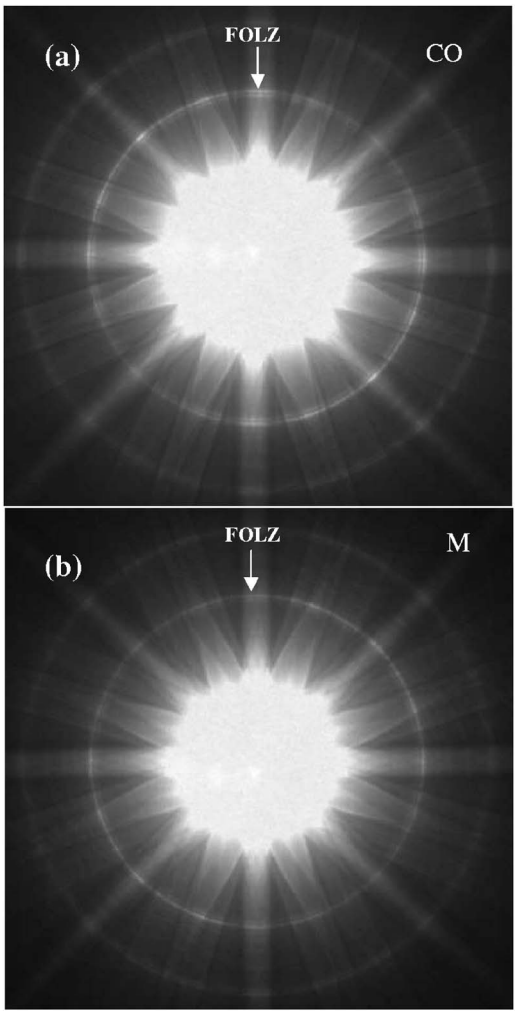

FIG. 7. Convergent beam electron diffraction (CBED) patterns taken along the [010] zones of charge-ordered (a) and monoclinic (b) phases. The FOLZ rings indicated by arrows were used to measure the b parameters of the corresponding phases.

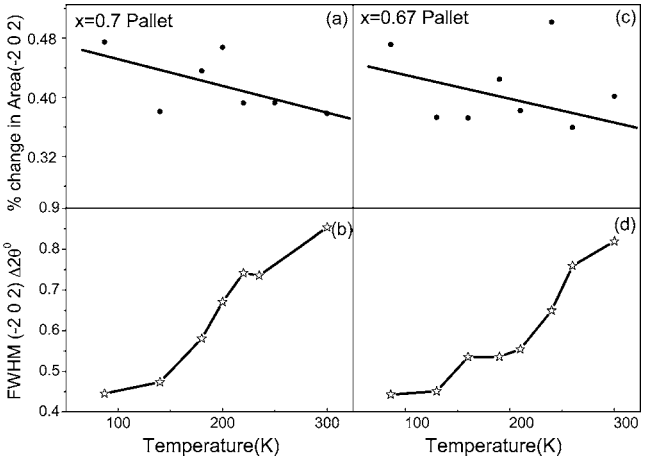

FIG. 8. Graphs showing the temperature variation of the integrated intensity and the FWHM of the $(\bar{2}02)$ peak of the M phase. A nominal increase in the volume fraction and coarsening of the grains of the M phase can be seen.

IV. DISCUSSION AND CONCLUSION

From the XRD results presented in Figs. 1–5, it is vividly clear that the observed coexistence of M and CO phases is irrespective of sample temperature. It is also clear that coexistence occurs in the pellet samples only and is absent from the corresponding powdered samples. Employing multiple profile fittings, as shown in Fig. 4, temperature variation of the area and full width at half maximum (FWHM) of $(\bar{2}02)$ peak of the M phase was determined. Figure 8 presents these analyses for $x=0.67$ and 0.7 samples. The occurrence of the M phase only in the pellets, and its almost complete absence from the powdered version of the sample obtain from the same pellets, even at 87 K, clearly reveals that the reported coexistence[7,8] of the M and CO phases at low temperatures is basically due to the presence of strain in the samples. This is corroborated by TEM results too. The occurrence of exactly reproducible microstructures at low temperatures and the absence of compositional inhomogeneity between the micron-sized grains should be related with some long-range lattice strain in the sample.[6,20] This is quite likely to be present in pellets. The pellets of these compounds are usually made at high pressures followed by sintering at high temperatures. When these are cooled to room temperature, the strain gets locked in the grain boundary network. When these pellets are crushed to nearly single grains, the grain boundary network breaks and the locked-in strain gets relaxed. It should be noted that even if some undetectable amount of chemical inhomogeneity is present, it would not vanish during gentle crushing for just 2–3 min and would persist even in powders. Thus the observed M phase in pellets is due to the strain present in them and not due to any chemical inhomogeneity. To clarify the effect of strain present in pellets at room temperature, a SAD pattern was taken from the same common region from which the diffraction pattern shown in Fig. 6(f) was taken. An enlarged view of this is shown in Fig. 9. Occurrence of elongation of diffraction spots exactly in the same direction as that of the monoclinic splitting, as shown in Fig. 6(f), clearly reveals the presence of strained regions resulting in the monoclinic distortion. It is this distortion that has appeared as a broad shoulder in the XRD profiles. By comparing the room-temperature XRD peaks of $(\bar{2}02)$ of the M phase and (202/040) of the *Pnma* phase, collected in two different but unique orientations of the pellet, we could show that the M phase is almost isotropically oriented in the pellet samples, see Fig. 10. From Figs. 8(a) and 8(c), it appears that volume fraction of M phase does show a nominal increase accompanied with coarsening of grains (decreasing FWHM) with decreasing temperature of pellet samples. Coarsening of the needle twins of the M phase in the a-c plane coexisting with the CO phase has been seen through TEM (Ref. 7) also. It should be noted that the strain is suspected even in single crystals, giving rise to reproducible microstructure in the scanning photoemission spectroscopic (PES) microscopy of coexisting metallic and insulating phases.[6]

At this juncture it would be imperative to compare the low-temperature TEM and XRD results of pellets. According

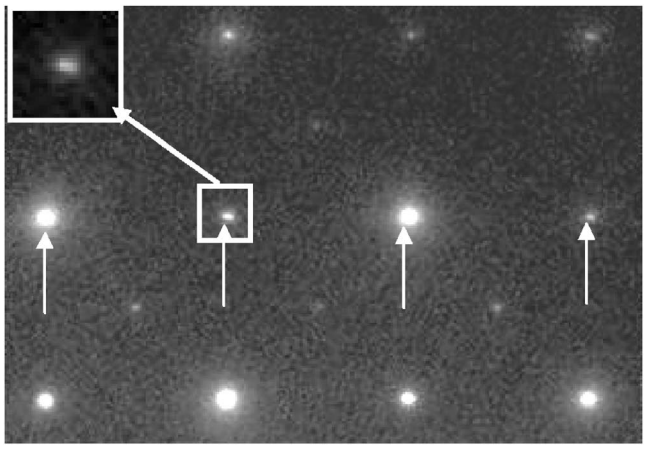

FIG. 9. Enlarged view of the electron diffraction pattern taken at room temperature from the same common region as that of the pattern shown in Fig. 6(f). The elongation of spots attribute to the presence of strain in the sample initiating monoclinic distortion of the neighboring region.

to the XRD results as shown in Fig. 8(c), the volume fraction of the M phase at ~109 K is ~40%. Thus, during TEM investigation at ~109 K, either at least every third grain should have been found to be of M phase or each grain should have shown the coexistence of M with CO phase with the volume fraction of ~40%. But surprisingly we could not find any such observation in an otherwise well-prepared TEM sample. CO was observed in every grain but the coexistence of M phase with CO, as shown in Fig. 6(d), was found in very few grains. A rough positive estimate of the volume fraction of the M phase, based on TEM observation, would no way exceed 5%. This observation also indicates the role of strain imposed by the grain boundary network on the coexistence of the M with the CO phase. The size of the grains is about ~5 μm. If such a large grain is thinned to ~1000 Å for making it electron transparent, most of the strain imposed by the grain boundary network will get relaxed[21] and therefore the number of grains exhibiting coexistence would decrease drastically or may even become vanishingly small.

Ahn *et al.*[16] have strongly indicated the importance of structural aspects such as strain for the multiphase coexistence, which act as templates for driving unique electronic and magnetic properties. Theoretically[16,22] and experimentally[23,24] it is now well established that intrinsic or extrinsic strains control the various physical properties of variety of complex oxides such as cuprates, manganites, ferroelastic martensites, and titanates. In the presence of strain, either external (pressure) or internal (chemical substitution), the electron-lattice coupling α_{ij} gets modified. It is approximately given by $\alpha_{ij}=\alpha_0\{1-\alpha\varepsilon_{ij}\}$;[22] here α_0 is the bare hopping integral, α is the coupling constant, and ε_{ij} represents the strain (lattice distortion variable). Thus it is clear that for any finite value of ε_{ij} the electron-lattice coupling reduces, decreasing the formation of polarons. This will lead to delocalization of carriers at a lattice site in manganite grains under strain. Delocalization will inhibit charge ordering. Thus the grain under strain will remain noncharged-ordered even below charge-ordering temperature (T_{CO}). When strain is removed by crushing the pellet sample to fine powder, the term ε_{ij} vanishes and hence we don't see any noncharge-ordered region, which is monoclinic in the present case. The observation of a noncharge-ordered phase with increasing monoclinicity (obliquity in the *a-c* plane) with decreasing temperature appears to be interplay of softening of some elastic modulus associated with the pseudocubic phase. In this regard, experimental (ultrasonic measurements) and theoretical work have been done by Hazama *et al.*[25–27] and Khomskii *et al.*[28] It has been shown that the transverse modes C_{44}, propagating along [100] of pseudo cubic (i.e., $[\bar{1}01]$ of *Pnma*) and $(C_{11}-C_{12})/2$, propagating along [110] of pseudocubic (i.e., [100] or [001] of *Pnma*) and the longitudinal mode C_{11}, all show anomalies in the above-mentioned elastic moduli at T_{CO}. From literature,[25–27] it is known that softening of $(C_{11}-C_{12})/2$ mode induces strain leading to tetragonal/orthorhombic distortions depending upon its coupling with the quadruple, and the C_{44}, mode propagating along [100] of the pseudocubic induces ε_{xy} strain, giving rise to a monoclinic distortion of the lattice.

The C_{44} mode although shows a monotonous increase but softens just above the T_{CO}, whereas the $(C_{11}-C_{12})/2$ mode shows monotonous decreasing trend above T_{CO} and hardens below T_{CO}. In our case of $La_{1-x}Ca_xMnO_3$ ($x>0.5$), this situation might be occurring for the grains showing charge-ordered superlattice peaks. But as described above, the region under strain will not undergo charge ordering even below T_{CO} due to strain-induced delocalization of carriers. The occurrence of noncharge-ordered monoclinic phase with $\beta=91.8\pm0.5°$ at 109 K (see Fig. 6) may be understood in terms of softening of the C_{44} mode. Usually the ε_{xy} strain induced due to softening of C_{44} is very tiny and therefore it will produce only a small tilt in the original orthogonal axis.

It should be noted that all the ultrasonic experiments for measuring elastic modulus have been done without applying

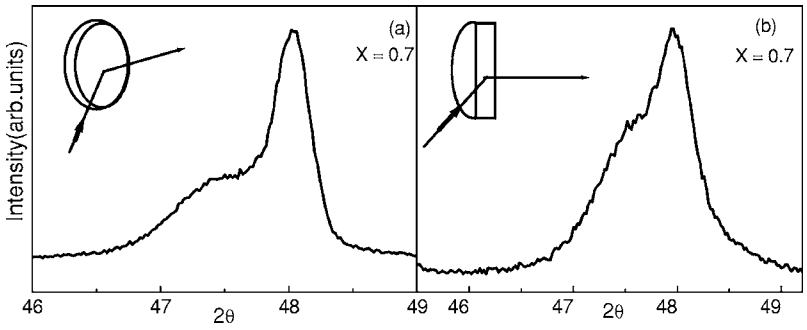

FIG. 10. The room-temperature XRD profiles corresponding to the pellet sample with $x=0.7$. These have been taken in two different orientations of the pellet as indicated in the insets. The area under the shoulder peak is nearly the same in both cases. This proves that the effect of the strain is isotropic.

any external strain. The presence of external strain (in our case being imposed by the grain boundary network) may modify the temperature dependence of various modes. The monotonous increasing trend of C_{44} with decreasing temperature may also get modify due to presence of external strain and it may show softening with decreasing temperature. The increasing monoclinicity with decreasing temperature, as realized during electron diffraction experiment, suggests this fact.

Thus based on the above observations, analysis, and discussions, it is concluded that the coexistence of monoclinic and charged-ordered phases in overdoped $La_{1-x}Ca_xMnO_3$ ($x>0.5$) manganites occurs due to the presence of strain in the bulk samples and not due to any chemical inhomogeneity. In polycrystalline pellets, this strain is self-imposed by the three-dimensional network of the grain boundaries. When properly crushed, the self-imposed strain gets relaxed and only charge-ordered phase occurs. This study indicates that most of the other coexistence in manganites—for example, antiferro-ferro and metal-insulator coexistence, which have been found in bulk ceramic samples—may be due to the presence of strain in these samples.

ACKNOWLEDGMENTS

The authors gratefully thank P. Chaddah, the director, and A. Gupta, the center director, of UGC-DAE-CSR Indore, D. D. Sarma, IISc Bangalore, and S. Sunder, IGCAR Kalpakkam, for their interest in the work and helpful discussions.

[1] T. A. Kaplan and S. D. Mahanti, *Physics of Manganites*, edited by T. A. Kaplan and S. D. Mahanti (Kluwer Academic/Plenum, New York, 1999).

[2] C. N. R Rao and B. Raveau, *Colossal Magnetoresistance Charge Ordering and Related Properties of Manganese Oxides*, edited by C. N. R. Rao and B. Raveau (World Scientific, Singapore, 1998).

[3] Y. Tokura, *Colossal Magneto-resistive Oxides*, edited by Y. Tokura (Gordon and Breach Science Publishers, New York, 2000).

[4] J. C. Loudon, N. D. Mathur, and P. A. Midgley, Nature (London) **420**, 797 (2002).

[5] M. Fath, S. Freisen, A. Menovsky, Y. Tomioka, J. Aarts, and J. A. Mydosh, Science **285**, 1540 (1999).

[6] D. D. Sarma Dinesh Topwal, U. Manju, S. R. Krishnakumar, M. Bertolo, S. La Rosa, G. Cautero, T. Y. Koo, P. A. Sharma, and S.-W. Cheon, Phys. Rev. Lett. **93**, 097202 (2004).

[7] J. C. Loudon and P. A. Midgley, Phys. Rev. B **71**, 220408(R) (2005).

[8] M. Pissas, I. Margiolaki, K. Prassides, and E. Suard, Phys. Rev. B **72**, 064426 (2005).

[9] P. W. Kolb, D. B. Romero, H. D. Drew, Y. Moritomo, A. B. Souchkov, and S. B. Ogale, Phys. Rev. B **70**, 224415 (2004).

[10] *Nanoscale Phase Separation and Colossal Magnetoresistance*, edited by Elbio Dagotto, Springer Series in Solid State Sciences, Vol. 136 (Springer, Berlin, 2003).

[11] T. V. Ramakrishnan, H. R. Krishnamurthy, S. R. Hassan, and G. Venketeswara Pai, Phys. Rev. Lett. **92**, 157203 (2004); H. R. Krishanamurthy, Pramana, J. Phys. **64**, 1063 (2005).

[12] N. D. Mathur and P. B. Littlewood, Solid State Commun. **119**, 271 (2001).

[13] A Moreo, S. Yunoki, and E. Dagotto, Science **283**, 2034 (1999).

[14] E. Dagotto, T. Hotta, and A Moreo, Phys. Rep. **344**, 1 (2001).

[15] J. Burgy, A. Moreo, and E. Dagotto,.Phys. Rev. Lett. **92**, 097202 (2004).

[16] K. H. Ahn, T. Lookman, and A. R. Bishop, Nature (London) **428**, 401 (2004).

[17] M. A. Fradkin J. Phys.: Condens. Matter **9**, 7925 (1997).

[18] P. R. Sagdeo, Shahid Anwar, and N. P. Lalla, Powder Diffr. **21**, 40 (2006).

[19] P. R. Sagdeo, Shahid Anwar, and N. P. Lalla, Solid State Commun. **137**, 158 (2006).

[20] J. Tao and J. M. Zuo, Phys. Rev. B **69**, 180404 (2004).

[21] S. Cox, E. Rosten, J. C. Chapman, S. Kos, M. J. Calderon, D. J. Kang, P. B. Littlewood, P. A. Midgley, and N. D. Mathur, Phys. Rev. B **73**, 132401 (2006).

[22] Jian-Xin Zhu, K. H. Ahn, Z. Nussinov, T. Lookman, A. V. Balatsky, and A. R. Bishop, Phys. Rev. Lett. **91**, 057004 (2003).

[23] Y. Moritomo, H. Kuwahara, Y. Tomioka, and Y. Tokura, Phys. Rev. B **55**, 7549 (1997).

[24] J. L. García-Muñoz, M. Amboage, M. Hanfland, J. A. Alonso, M. J. Martinez-Lope, and R. Mortimer, Phys. Rev. B **69**, 094106 (2004).

[25] H. Hazama, T. Goto, Y. Nemoto, Y. Tomioka, A. Asamitsu, and Y. Tokura, Phys. Rev. B **62**, 15012 (2000).

[26] H. Hazama, T. Goto, Y. Nemoto, Y. Tomioka, A. Asamitsu, and Y. Tokura, Phys. Rev. B **69**, 064406 (2004).

[27] H. Hazama, T. Goto, Y. Nemoto, Y. Tomioka, A. Asamitsu, and Y. Tokura, Physica B **312-313**, 757 (2002).

[28] D. I. Khomskii and K. I. Kugel, Phys. Rev. B **67**, 134401 (2003).